MULTI-MESSENGER EXTENDED EMISSION FROM THE COMPACT REMNANT IN GW170817

Maurice H.P.M. van Putten
Sejong University, 98 Gunja-Dong Gwangin-gu, Seoul 143-6%747, Korea; E-mail: mvp@sejong.ac.kr

Massimo Della Valle
Istituto Nazionale di Astrofisica, Osservatorio Astronomico di Capodimonte, Salita Moiariello 16, I-80131 Napoli, Italy

Amir Levinson
School of Physics and Astronomy, Tel Aviv University, 69978 Tel Aviv, Israel
Draft version October 29, 2019

ABSTRACT

GW170817/GRB170817A probably marks a double neutron star coalescence. Extended Emission $t_s \simeq (0.67 \pm 0.03)$ s post-merger shows an estimated energy output $\mathcal{E} \simeq (3.5 \pm 1)\% M_\odot c^2$ determined by response curves to power-law signal injections, where c is the velocity of light. It provides calorimetric evidence for a rotating black hole of $\sim 3M_\odot$, inheriting the angular momentum J of the merged hyper-massive neutron star in the immediate aftermath of GW170817 following core-collapse about or prior to t_s. Core-collapse greatly increases the central energy reservoir to $E_J \lesssim 1M_\odot c^2$, accounting for $\mathcal{E}$ even at modest efficiencies in radiating gravitational waves through a non-axisymmetric thick torus. The associated multi-messenger output in ultra-relativistic outflows and sub-relativistic mass-ejecta is consistent with observational constraints from the GRB-afterglow emission of GRB170817A and accompanying kilonova.

1. INTRODUCTION

GW170817 (Abbott et al. 2017a,b) is the first observation of a low-mass compact binary coalescence seen in a long duration ascending gravitational-wave chirp. By the accompanying GRB170817A identified by *Fermi*-GBM and INTEGRAL (Connaughton 2017; Savchencko et al. 2017; Goldstein et al. 2017; Pozanenko et al. 2018; Kasliwal et al. 2017) it represents the merger of a neutron star with another neutron star (NS-NS) or companion hole (NS-BH) with a chirp mass of about one solar mass. Potentially broad implications of the first has received considerable attention for our understanding of the origin of heavy elements (Kasen et al. 2017; Smartt et al. 2017; Pian et al. 2017; D'Avenzo et al. 2017) and for entirely novel measurements of the Hubble constant (Guidorzi et al. 2017; Freedman 2017).

By chirp mass, the nature of GW170817 is inconclusive in the absence of observing final coalescence at high gravitational-wave frequencies (Coughlin & Dietrich 2019). For NS-NS coalescence, numerical simulations (e.g. Baiotti & Rezzolla 2017) show gravitational radiation to effectively satisfy the canonical model signal of binary coalescence in a run-up to about 1 kHz, beyond which the amplitude levels off and ultimately decays as the two stars merge into a single object at a maximal frequency ∼3 kHz. In contrast, NS-BH mergers include tidal break-up (Lattimer & Schramm 1976). In a brief epoch of hyper-accretion, the black hole would be near-extremal with a remnant of NS debris to form a torus outside its Inner Most Stable Circular Orbit (ISCO). This process is marked by gravitational radiation switching off early on at a frequency 500-1500 Hz (Vallisneri 2000; Faber 2009; Etienne et al. 2009; Ferrari et a. 2010) and possibly quasi-normal mode oscillations at yet higher frequencies (e.g Yang et al. 2018).

Here, we report on the energy output $\mathcal{E}$ in gravitational radiation post-merger, that appears as a descending chirp of Extended Emission marking spin-down of a compact remnant to binary coalescence at a Gaussian equivalent level of confidence of 4.2σ (van Putten & Della Valle 2019). We give a robust estimate of $\mathcal{E}$ by response curves determined by signal injection experiments in data of the LIGO detectors at Hanford (H1) and Livingston (L1). $\mathcal{E}$ introduces a new calorimetric constraint that may break the degeneracy of a NS or BH central engine.

$\mathcal{E}$ reported here points to core-collapse of the merged NS produced in GW170817, inheriting its angular momentum J while greatly increasing the associated spin-energy E_J through collapse to a Kerr BH (Kerr 1963).

After our injection experiments were initiated, we learned of an independent analysis of energy considerations by single-template injections, pointing qualitatively to similar energies without, however, identifying the origin of our Extended Emission (Oliver et al. 2019).

2. $\mathcal{E}$ FROM PIPELINE RESPONSE CURVES

We set out to determine response curves of our search pipeline by signal injections into LIGO data (Vallisneri et al. (2014); Figs. 1-2), including whitening, butterfly filtering and image analysis of merged (H1,L1)-spectrograms (Appendix). Whitening is by normalizing the Fourier spectrum over an intermediate bandwidth of 2 Hz, bringing about GW170817 more clearly than without whitening (van Putten & Della Valle 2019).

We recall that GW170817 is observed as an *ascending chirp* signifying the merger of two compact stars with time-of-coalescence $t_c = 1842.43$ s followed by GRB170817A across a gap of 1.7 s. In our injection experiments to LIGO data, we include a model DNS with the same chirp mass $\mathcal{M}_c = 1.188M_\odot$ of GW170817 (Fig. 2) at time-of-coalescence about 1818 s, producing two ascending chirps side-by-side (Fig. 3). A DNS is de-
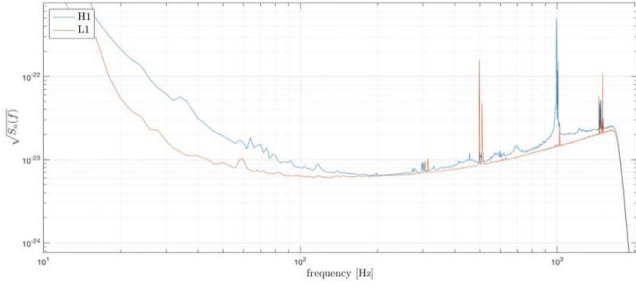
FIG. 1.— H1 and L1 detector noise shown by the square root of spectral energy density $S_n(f)$ (at reduced sampling rate 4096Hz with glitch in L1 removed by LIGO) for an epoch of 2048 s containing GW170817 (top panel). Spikes are violin modes associated with suspension of optics. Frequencies up to about 1700 Hz can be used in injection experiments. H1 and L1 detector noise is very similar during GW170817.

scribed by binary masses M_1, M_2, $\mu = M_1 M_2 / M$, $M = M_1 + M_2$, at orbital separation a and orbital frequency $\Omega \simeq c\sqrt{R_g/a^3}$ ($a >> R_g$), where $R_g = GM/c^2$ is the gravitational radius of the system, given the velocity of light c and Newton's constant G. This merger chirp has a quadrupole gravitational-wave frequency $f_{GW} = \pi^{-1}\Omega$,

$$f_{GW}(t) = A(t_c - t)^{-\frac{3}{8}} \quad (t < t_c), \qquad (1)$$

$[A] = \mathrm{s}^{-5/8}\,\mathrm{Hz}$, with strain $h(t) = (4\mu/D)\,(M\Omega)^{\frac{2}{3}}$, $h(t) \simeq 1.7 \times 10^{-22}\,(M/3M_\odot)\,(D/40\,\mathrm{Mpc})^{-1}\,(f_{GW}/250\,\mathrm{Hz})^{\frac{2}{3}}$ and $L_{GW} = (32/5)\,(\mathcal{M}_c\Omega)^{10/3}\,L_0$, where $L_0 = c^5/G \simeq 200,000 M_\odot c^2 \mathrm{s}^{-1}$ (e.g. Ferrari et a. 2010). For GW170817, $A \simeq 138\,\mathrm{s}^{-5/8}\,\mathrm{Hz}$. Up to 260 Hz in both H1 and L1, L_{GW} reaches $1.35 \times 10^{50}\mathrm{erg\,s}^{-1} \simeq 7.5 \times 10^{-5} M_\odot c^2\,\mathrm{s}^{-1}$, i.e., $4 \times 10^{-10} L_0$. While small compared to $10^{-5}L_0$ of GW150914 at similar frequency, GW170817 produced the largest strain observed by its proximity of $D \simeq 40$Mpc. It emitted $E_0 = 0.43\% M_\odot c^2$ over 200-300 Hz with $h = 1.4 - 1.8 \times 10^{-22}$ over $\Delta t \simeq 0.25\,\mathrm{s}$ across $74\,\mathrm{km} < r < 97\,\mathrm{km}$ assuming $M_1 = M_2$.

A merged (H1,L1)-spectrogram shows Extended Emission post-merger below 700 Hz in the form of an exponential feature

$$f_{GW}(t) = (f_s - f_0)e^{-(t-t_s)/\tau_s} + f_0 \quad (t > t_s) \qquad (2)$$

with the observed $\tau_s = 3.01 \pm 0.2\,\mathrm{s}$, $t_s = 1843.1\,\mathrm{s}$, $f_s = 650\,\mathrm{Hz}$ and $f_0 = 98\,\mathrm{Hz}$. For illustrative purposes, we note the isotropic equivalent strain $h = L_{GW}^{1/2}/(\Omega D)$ (in geometrical units, $c = G = 1$) for the chirp mass of a small quadrupole mass-moment $\zeta = \delta m/M$ gives $h(t) \simeq 2.7 \times 10^{-23}\,(\zeta/3\%)\,(D/40\,\mathrm{Mpc})^{-1}\,(f_{GW}/650\,\mathrm{Hz})^{2/3}$, $L_{GW} \simeq 2 \times 10^{52}\,(\zeta/3\%)^2\,(10M/r)^5\,\mathrm{erg\,s}^{-1} \simeq 1\% M_\odot c^2/\mathrm{s}^{-1}$.

We next use phase coherent injections with frequency evolution (2) (Supplementary Data). No change in results below are found upon including phase incoherence by a Poisson distribution of random phase jumps over intermediate time scales, down to the duration $\tau = 0.5\,\mathrm{s}$ of our butterfly templates. $\tau = 0.5$ appears intrinsic, as the Extended Emission feature tends to fade out as τ
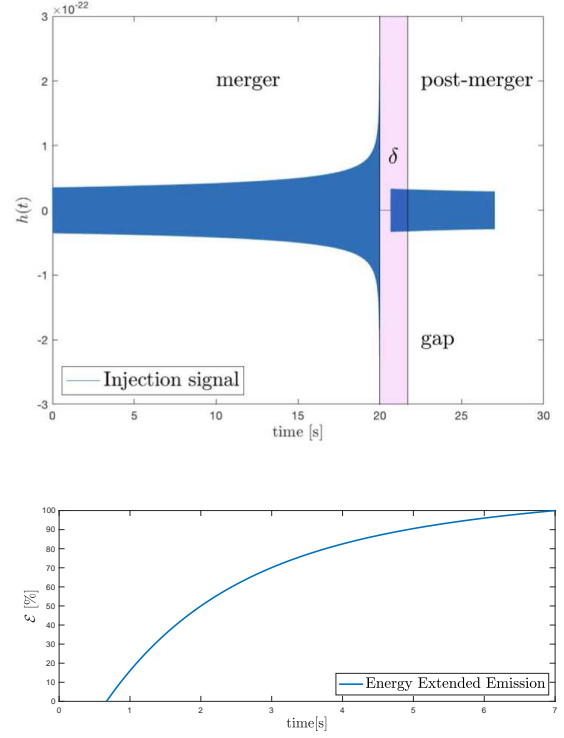

FIG. 2.— Injection signal comprising a DNS merger and a post-merger branch separated by a delay $\delta = 0.67\,\mathrm{s}$ inside the gap of 1.7 s between GW170817 and GRB170817A. The post-merger signal has a duration of 7 s at with relatively flat strain $h \propto f^\alpha$ ($\alpha = 0.1$).

approaches 1 s.

The total energy output $\mathcal{E} = \int_0^T L_{GW} dt$ is computed numerically as sums $\mathcal{E} = E_0 K^{-1} \sum \nu_i^2 h_i^2$ (samples at t_i, $i = 1, 2, .., n$) covering a post-merger interval of duration T, where $K = \sum \nu_{0,j}^2 h_{0,j}^2$ (samples at t_j, $j = 1, 2, \cdots, m$) is a reference sum with energy E_0 over a duration T_0, where $\nu_i = f_{GW}(t_i)$ denotes gravitational-wave frequency. E_0 is conform quadrupole emission in the same orientation of the progenitor binary by conservation of orbital-to-spin angular momentum in transition to its remnant. Blind to any model in particular, we consider injections with power-law strain $h \propto f^\alpha$ with $T = 7\,\mathrm{s}$.

Fig. 3 shows the outcome of a signal-injection alongside GW170817EE after a calibration $C_h = 0.7$ for observed-to-true strain due to non-ideal H1 and L1 detector orientations relative to GW170817. Extended to multiple injections, results show there is no interference with the merger signal or with one another.

Fig. 4 shows our estimated response curves $\chi(\mathcal{E})$ for $h \propto f^\alpha$ ($0.1 \leq \alpha \leq 1.0$). By $\hat{\chi} \simeq 7.2$ of the Extended Emission to GW170817, we infer

$$\mathcal{E} \simeq (3.5 \pm 1)\% M_\odot c^2, \qquad (3)$$

For the descending chirp at hand (2), $\mathcal{E}$ mostly derives early on at high f_{GW} with $L_{GW} \lesssim 1\% M_\odot c^2\mathrm{s}^{-1}$ (Fig. 2).

3. ENHANCED E_J IN COLLAPSE TO A BLACK HOLE

$\mathcal{E}$ in (3) is a significant amount of energy, exceeding the merger output observed up to about 300 Hz, emitted as a

descending chirp over a secular time scale of seconds with $f_{GW} < 700\,\mathrm{Hz}$ far below the characteristic frequency $c/R_S \simeq 30\,\mathrm{kHz}$ of the Schwarzschild radius $R_S = 2R_g$. Important energies also appear in GRB170817A and mass-ejecta (e.g. Mooley et al. 2018a,b). Of these, $\mathcal{E}$ and f_{GW} will serve as primary observational constraints on the remnant, i.e., E_J of a rapidly spinning merged NS or rotating BH.

While a long-lived NS might be luminous in gravitational radiation through a baryon-loaded magnetosphere (Appendix), its spin-frequency $f_s = (1/2)f_{GW}$ inferred from our Extended Emission is less than one-fifth the break-up spin-frequency of about 2 kHz. This modest initial spin limits E_J to below $0.5\% M_\odot c^2$ and probably somewhat less based on more stringent limits (e.g. Haensel et al. 2009; Oliver et al. 2019).

However, E_J greatly increases by core-collapse of the merged NS in the immediate aftermath of GW170817, here at time of core-collapse about or prior to $t_s = 0.67(\pm 0.03)\,\mathrm{s}$ post-merger (Fig. 3), where the 30ms refers to our time-step in t_s. By the Kerr (1963) metric,

$$E_J = 2Mc^2 \sin^2(\lambda/4) \lesssim 1 M_\odot c^2 (M/3M_\odot) \qquad (4)$$

in terms of $a/M = \sin\lambda$, $J = a\sin\lambda$. This potentially enormous energy reservoir amply accounts for $\mathcal{E}$ even at modest efficiency η, provided a mechanism is in place to tap and convert E_J into gravitational radiation. Moderate frequencies $f_{GW} < 700\,\mathrm{Hz}$ can be realized in catalytic conversion into quadrupole emission by a non-axisymmetric disk or torus, sufficiently wide or geometrically thick. Exhausting E_J, a descending chirp results due to expansion of the ISCO during black hole spin-down.

4. $\mathcal{E}$ ESTIMATE FROM BLACK HOLE SPIN-DOWN

To add some concreteness, we estimate η in spin-down of an initially rapidly rotating BH, losing J to matter in Alfvén waves through an inner torus magnetosphere (van Putten 1999, 2001). By heating, a non-axisymmetric thick torus is expected to generate frequencies correlated to but below those of a thin torus about the ISCO (Coward et al. 2002). In geometrical units, an extended torus produces emission from an orbital radius $r \equiv z R_g$ at twice the local orbital frequency, i.e., $f_{GW} \simeq c\pi^{-1}\sqrt{R_g/r^3}$. Asymptotic scaling relations for large radii (modest η) (van Putten & Levinson 2003) show $L_{GW} \sim 10^{52}\mathrm{erg\,s}^{-1}$ for a non-axisymmetric torus with mass ratio $\sigma = M_T/M \simeq 0.1$. Accompanying minor output is in MeV-neutrinos and $E_w \simeq \eta^2 E_J$ in magnetic winds (van Putten & Levinson 2002, 2003) - *most of E_J is dissipated unseen in the event horizon, increasing area by Bekenstein-Hawking entropy (van Putten 2015)*. The observed $150\,\mathrm{Hz} < f_{GW} < 700\,\mathrm{Hz}$ indicates an effective radius of a quadrupole mass moment initially about three times the ISCO radius (Fig. 5), indicating a relatively thick torus. f_{GW} decreases with z with expansion of the ISCO during black hole spin-down.

By numerical integration of this spin-down process, catalytic conversion of E_J gives (Fig. 5)

$$\mathcal{E} \simeq \langle \eta \rangle E_J \simeq 3.6 - 4.3\% M_\odot c^2 \qquad (5)$$

for canonical values of initial a/M, depending somewhat on the start frequency $f_s = 600 - 700\,\mathrm{Hz}$, consistent with

(3) inferred from $\chi(\mathcal{E})$.

The model estimate (5) uses effective values of disk mass m and K throughout. This does not readily predict $h(f_{GW})$ or the observed exponential feature (2), as m and K will be time-dependent and vary with z. Use of effective mean values is only for our present focus on total energy output.

While the nature of GW170817 by the chirp up to 300 Hz is somewhat inconclusive (Coughlin & Dietrich 2019), $\mathcal{E}$ provides a novel calorimetric constraint on its remnant. $\mathcal{E}$ in (3) challenges a hyper-massive NS (Oliver et al. 2019) yet is naturally accommodated by (5) in core-collapse to a Kerr BH.

In converting E_J, $\mathcal{E}$ is accompanied by MeV-neutrinos and magnetic winds (van Putten & Levinson 2003) consistent with evidence for black hole spin-down in normalized light curves of long GRBs (van Putten 2012).

5. MULTI-MESSENGER EXTENDED EMISSION

Starting with the merged NS from a DNS, a time-of-collapse about or prior to $t_s \simeq 0.67(\pm 0.03)\,\mathrm{s}$ (Fig. 3) appears consistent - perhaps in mild tension - with the recently estimated time-of-collapse $0.98^{+0.31}_{-0.26}\,\mathrm{s}$ based on jet propagation times and mass of blue-ejecta (Gill et al. 2019).

Sustained by Alfvén waves outwards over an inner torus magnetosphere, a torus developing a dynamo with magnetic field $B = O(10^{16})\,\mathrm{G}$ limited by dynamical stability over the lifetime of black hole spin (van Putten & Levinson 2003) gives a characteristic time scale for the lifetime of rapid spin of the BH and hence of the BH-torus system,

$$T_s \simeq 1.5\,\mathrm{s}\left(\frac{\sigma}{0.1}\right)^{-1}\left(\frac{z}{6}\right)^4\left(\frac{M}{3M_\odot}\right), \qquad (6)$$

consistent with the duration T_{90} (90% of gamma-ray counts over background) of GRB170817A. Over this secular time scale, the BH gently relaxes towards a nearly Schwarzschild BH as the ISCO expands. A relatively baryon-poor environment of the BH is ideally suited for it to also launch an ultra-relativistic baryon-poor jet within a baryon-rich disk or torus wind with (van Putten & Levinson 2003)

$$E_j \simeq \frac{E_J}{4z^4} \simeq 5 \times 10^{50}\mathrm{erg}, E_w \simeq \eta^2 E_J \simeq 4 \times 10^{51}\mathrm{erg}, (7)$$

consistent with $E_j \sim 10^{49-50}\mathrm{erg}$ and $E_k = (1/2)M_{ej}v^2 \simeq 4.5 \times 10^{51}$ in the relativistic ejecta of GRB170817A and $M_{ej} \simeq 5\% M_\odot$ of mass ejecta at mildly relativistic velocities $v \simeq 0.3c$ (Mooley et al. 2018a,b). Emission terminates abruptly as the remnant torus collapses onto the black hole when $\Omega_H \simeq \Omega_T$ ($f_{GW} \simeq 10^2\,\mathrm{Hz}$).

6. CONCLUSIONS

$\mathcal{E} \simeq (3.5 \pm 1)\% M_\odot c^2$ in Extended Emission measured by $\hat{\chi}(\mathcal{E})$ through signal injections (Fig. 4) gives a powerful calorimetric constraint on the central engine. This outcome points to a Kerr BH formed in core-collapse of the merged NS in the immediate aftermath of GW170817.

At $f_{GW} < 700\mathrm{Hz}$, our $\mathcal{E}$ is consistent with post-merger bounds of LIGO (Abbott et al. 2017c, between dashed
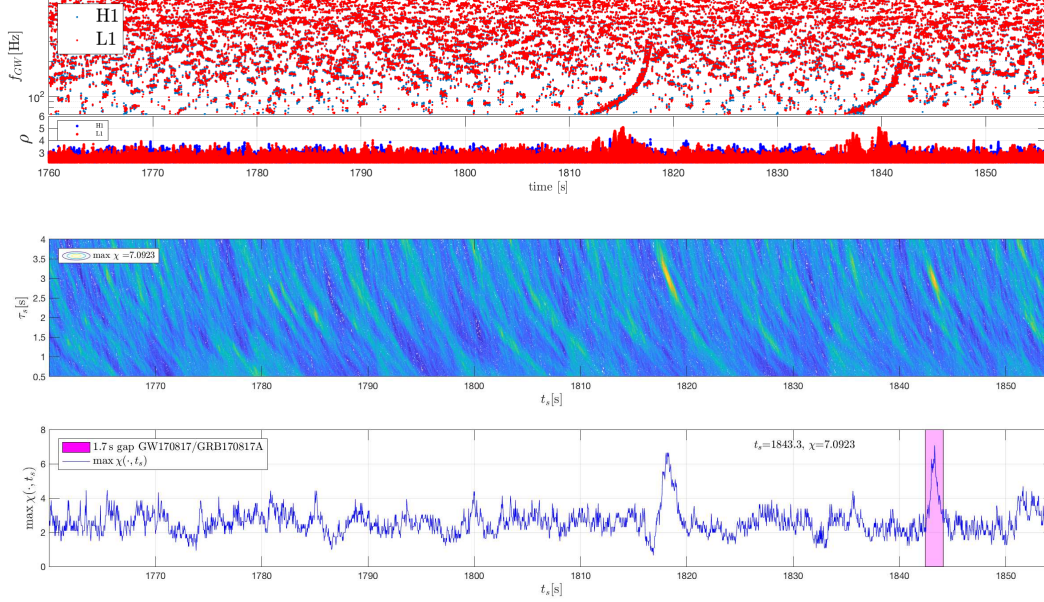
FIG. 3.— (Upper panel.) (H1,L1)-spectrogram merged by frequency coincidences of butterfly filtering showing GW170817 ($t_c = 1842.43$ s) alongside a model signal ($t_c \simeq 1818$ s). GW170817 appears with $\mathcal{E} \simeq 3\% M_\odot c^2$ in Extended Emission. Included is $\rho = \sqrt{\mathrm{SNR}}$ in the tail > 2 of butterfly output of H1 and L1. (Lower panel.) χ-image analysis of Extended Emission in the (H1,L1)-spectrogram over parameters (t_s, τ_a) for initial and final frequencies $(f_s, f_0) = (650, 98)$ Hz (upper panel) with similar signal strength of Extended Emission of signal injection to that of GW170817 ($t_s = 0.67(\pm 0.03)$s) measured by peak-value of the indicator χ.
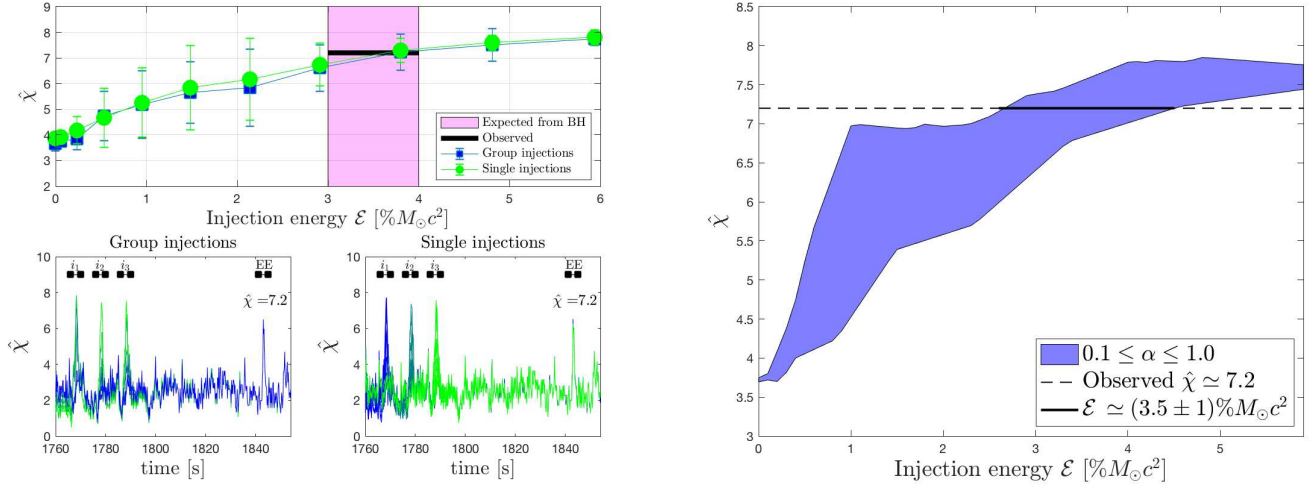

FIG. 4.— (Left panel.) Response peaks $\hat{\chi}(\mathcal{E})$ of signal injections $h \propto f^\alpha$ ($\alpha = 0.1$) in a merged (H1,L1)-spectrogram covering GW170817 by the indicator function $\hat{\chi}$ in χ−image analysis as a function of energy input $\mathcal{E}$. The response curve (green, blue curves; top panel) determined by injections at instances (i_1, i_2, i_3) about 1 min before GW170817 (lower panels) is the same by grouped (left bottom) or single (right bottom) injections, demonstrating non-interference between different signals. Color (blue to green) indicates injection strength in group injections and injection position in single injections. Scatter in $\chi(E)$ by noise fluctuations appears least at i_1. (Right panel.) Extended Emission to GW170817 is observed at $\hat{\chi} \simeq 7.2$ (blue dashed) intersected by $\hat{\chi}(\mathcal{E})$ from i_1 to power-law injections $h \propto f^\alpha$ ($\alpha = 0.1, 0.2, \cdots 1.0$) (blue filled).

lines $E_{gw} = 0.01 - 0.1 M_\odot c^2$ in Fig. 1) and Oliver et al. (2019). With E_J of a Kerr BH, concerns of Oliver et al. (2019) on detectability of Extended Emission are unfounded. Accurate time-integration of the complex scaling $L_{GW} \propto (f_{GW}[h/C_h])^2$ highlights a need for measurement by signal injection, for which a one-frequency estimate of h_{H1} alone (van Putten & Della Valle 2019) now appears inadequate.

Core-collapse greatly enhances E_J in J inherited from the merged NS up to about $1 M_\odot c^2$ in a $\sim 3 M_\odot$

BH. It amply accommodates $\mathcal{E}$ even at modest efficiencies in conversion to $\mathcal{E}$ over durations of seconds (Fig. 5). Accompanying minor emissions (7) in mass ejecta from the torus and ultra-high energy emission from the BH agree quantitatively with observational constraints on the associated kilonova and GRB170817A. GW170817 is too distant, however, to probe any MeV-neutrino emission (Bays et al. 2012) its MeV-torus (van Putten & Levinson 2003).

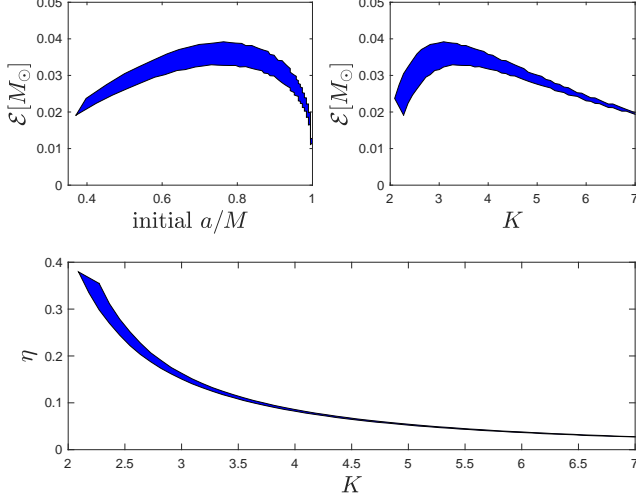Conceivably, EE does not completely exhaust E_J, per-

FIG. 5.— (Model prediction of $\mathcal{E}$ in a descending chirp from a non-axisymmetric torus of effective radius K times the ISCO radius around a black hole of initial mass $M_0 = 3M_\odot$, converting E_J into gravitational radiation at moderate efficiencies η. The boundaries of the thick curve refers to gravitational-wave frequencies $f_s = 600 - 700$Hz at start-time t_s.

At improved sensitivity, LIGO-Virgo O3 observations may significantly improve on our ability to identify the nature of binary mergers involving a NS - including the tidal break-up in a NS-BH merger - and their remnants that might also be found in core-collapse supernovae and, possibly, accretion induced collapse of white dwarfs.

Supporting Data:

WInjection.m, whitening and signal injection (Fig. 2), DOI 10.5281/zenodo.2613112
EEE.m, estimated energy and efficiency of Extended Emission (Fig. 5), DOI 10.5281/zenodo.2613105

mitting low-luminosity latent emission including minor output in baryon-loaded disk winds and low-luminosity jets. While outside the present scope, such might be an alternative to the same from a long-lived NS remnant needed to account for ATo2017gfo (Ai et al. 2018; Li et al. 2018; Yu et al. 2018; Piro et al. 2019).

APPENDIX

Our broadband extended gravitational-wave emission (BEGE) pipeline aims for un-modeled ascending and descending chirps with a choice of intermediate time-scale of phase-coherence $0 < \tau \lesssim 1$s, expected from extreme transient events exhausting E_J of their central engine in seconds:

- Butterfly filtering is matched filtering against a bank of time-symmetric chirp-like templates of intermediate duration τ, densely covering a domain in $(f(t), |df(t)/dt| \geq \delta)$ for some choice of $\delta > 0$. Single detector spectrograms are extracted as scatter plots of correlations $\rho(t, f_c)$ between data segments (here, of 32 s duration) and time-symmetric chirp-like templates with central frequency f_c.

- To reduce noise in deep searches ($\kappa = 2$), spectrograms are merged by frequency coincidences ($|f_{c,H1} - f_{c,H2}| < \Delta f$) conform causality: Δf is about $|df(t)/dt| \, \delta t$, where $\delta t = 10$ms is the (maximal) signal propagation time between H1 and L1. We obtain satisfactory results with $\Delta f = 10$Hz (Fig. 3).

- Candidate features (Fig. 3) are evaluated by counting 'hits:' $\chi(\rho > \kappa\sigma)$ by H1&L1 over strips about a given family of curves - normalized to $\hat{\chi}$. For Extended Emission feature to GW170817, we use (2), giving $\hat{\chi}(t_s, f_s, f_0, \tau_s)$. The strip is of finite width ($\Delta f = 10$Hz, $\Delta t = 0.1$s), discretized with $\Delta t_s = 0.030$s and, for background statistics, over $N = 16$ steps in each parameter gathered from 1956s of clean LIGO data in a scan over a total of 256M parameters ($N^3 = 4096$, $\Delta t_s = 30$ms, van Putten & Della Valle (2019)).

The merged NS produced by GW170817 may briefly emit GWs through a magnetosphere with field B, baryon-loaded with M_b by dynamical mass ejecta and MeV-neutrino winds (e.g. Perego et al. 2014), by a quadrupole moment μ along its magnetic spin-axis misaligned with J (Kalapotharakos et al. 2012), extending out to l of its light cylinder. At Alfvén velocity $c_A = B/\sqrt{4\pi\rho}$, $B = B_{16}10^{16}$G with matter density ρ, μ greatly exceeds that of B in vacuum (Hacyen 2017). In geometrical units ($c = G = 1$), the polar flux axis radiates like a rod with (Wald 1984) $L_{GW} = (32/45)\mu^2\Omega^6 \simeq (32/45)(m\Omega)^2$ with $\mu = ml^2$. A star of mass M, radius R, Newtonian binding energy $W = M^2/(2R) \simeq 0.15$ generally satisfies $M >> W >> E_J >> E_{turb} >> E_B$ for turbulent motions E_{turb} and $E_B = (1/6)B^2R^3$. Hence, $E_B = (E_{rot}/W)(E_{turb}/E_{rot})(E_B/E_{turb})W \simeq 10^{-4}M$ for fiducial ratios of 0.1 for each factor with corresponding $B \simeq 4 \times 10^{16}$G. M_b enhances $m \simeq f_B E_B$ by $2\beta_A^{-2}$, $\beta_A = c_A/c$, where $f_B \simeq 0.5$ for a dipole field. Accordingly, $L_{GW} \simeq (32/45)\left(m\Omega\beta_A^{-2}\right)^2 \simeq 2 \times 10^{52}\left(B_{16}/(\beta_A/0.1)\right)^4 (f_s/350\text{Hz})^2$ erg s^{-1} at rapid spin when l is a few times R. Such burst will be short by canonical bounds on E_J of a NS.

E_J increases dramatically in continuing core-collapse to a BH. A numerical estimate of $\mathcal{E}$ derives from catalytic conversion of $E_J = 2M\sin^2(\lambda/2) \lesssim 0.29M$ at $a/M = \sin\lambda$ (non-extremal) at modest efficiency at orbital angular velocity $\Omega_T = \pi f_{GW}$ relative to $\Omega_H = \tan(\lambda/2)/(2M)$ of the BH. The estimated initial frequency of $\sim 744\,\mathrm{Hz}$ at time-of-coalescence t_c inferred from $t_s = 0.67\,\mathrm{s}$ is below the orbital frequency at which the stars approach the ISCO of the system mass, about $1100\,\mathrm{Hz}$ at $r \simeq 16$ km. At this point, an equal mass DNS has $a/M = 0.72 < 1$ consistent with numerical simulations (e.g. Baiotti & Rezzolla 2017), allowing collapse to a $\sim 3M_\odot$ Kerr BH with $E_J \simeq 24\% M_\odot c^2$. For a torus radius K times the ISCO radius, Fig. 5 shows the result of integration of the equations describing spin-down (Supplementary Data) with a $\mathcal{E} \simeq 3.6 - 4.3\% M_\odot$ at aforementioned canonical initial values a/M, subject to the observed gravitational-wave frequency $600\,\mathrm{Hz} < f_{GW} < 700\,\mathrm{Hz}$ at $t_s = 0.67\,\mathrm{s}$ post-merger - consistent with (3).

REFERENCES

Abbott, B.P., Abbott, R., Abbott, T.D., et al., 2017a, Phys. Rev. Lett., 119, 161101

Abbott, B.P., Abbott, R., Abbott, T.D., et al., 2017b, Astrophys. J. 848, L13

Abbott, B.P., et al., 2017, ApJ, 851, L16

Ai, S., Gau, He, Dai, Z.-G., Wu, X.-F., Li, A., Zhang, B., & Li, M.-Z., ApJ, 860, 57 (2018)

Baiotti, L., & Rezzolla, L. 2017, RPPh, 80, 096901

Bays, K., et al., 2012, Phys. Rev. D, 85, 052007

Connaughton, V. 2017, GCN, 21505

Coughlin, M. & Dietrich, 2019, arXiv:1901.06052v1

Coward, D.M., van Putten, M.H.P.M., & Burman, R.R., 2002, ApJ, 580, 1024

D'Avanzo, E., Benetti, S., Branchesi, M., Brocato, E., et al, 2017, Nat., 551, 67

Etienne, Z.B., Liu, Y.T., Shapiro, S.L., and Baumgarte, T.W., 2009, Phys. Rev. D 79, 044024

Faber, J.A., 2009, Class. Quant. Grav., 26, 114004

Ferrari, V., Gualtieri, L., & Pannarale, F., 2010, Phys. Rev. D, 81, 064026

Freedman, W. L. 2017, NatAs, 1, 0121

Gill, R., Nathanail, A., & Rezzolla, L., 2019, arXiv:1901.04138v1

Goldstein, A. et al., 2017, Astrophys. J. 848, L14

Guidorzi, C., Margutti, R., Brout, D., Scoling, D., Fong, W., et al., 2017, ApJ, 851, L36

Hacyan, S., 2017, Rev. Mex. Fis. 63, 466

Haensel, P., Zdunik, J. L., Bejger, M., et al. 2009, A&A, 502, 605

Kalapotharakos, C., Kazanas, D., Harding, A., & Contopoulos, I., 2012, ApJ, 749, 2

Kasliwal, M.M., Nakar, E., Singer, L.P., 2017, Science, 358, 1559

Kasen, D., Metzger, B., Barnes, J., et al., 2017, Nat., 551, 80

Kerr, R.P., 1963, Phys. Rev. Lett., 11, 237

Lattimer, J.M., & Schramm, D.N., 1976, ApJ, 210, 549

Li, S.-Z., Liu, L.-D., Yu, Y.-W. & Zhang, B., 2018, ApJ, 861, L12

Metzger B. D., Thompson T. A., Quataert E., 2018, ApJ, 856, 101

Oliver, M., Keitel, D., Miller, A., et al., 2019, arXiv:1812.06724

Perego, A., Rosswog, S., Cabezón, R.M., et al., 2014, MNRAS, 443, 3134

Pian, E., D'Avanzo, P.,Benetti, S., Branchesi, M., Brocato, E., et al. 2017, Nat., 551, 67

Piro, L., Troja, E., Zhang, B., et al., 2019, MNRAS, 483, 1912

Pozanenko, A.S., Barkov, M.V., Minaev, P.Y., et al., 2018, ApJ, L30

Mooley, K.P., Deller, A.T., Gottlieb, O., et al., 2018, Nat. 554, 207

Mooley, K.P., Deller, A.T., Gottlieb, O., et al., 2018, Nat. 561, 355

Savchenko, V., Ferrigno, C. , Kuulkers, E., et al., 2017, ApJ, 848, L15

Siellez, K., Boër, M., & Gendre, B., 2013, MNRAS, 437, 639

Smartt, S.J., Chen, T.-W., Jerkstrand, A., Couthlin, M., Kankare, E., et al., 2017, Nat., 551, 75

Vallisneri, M., 2000, Phys. Rev. Lett., 84, 3519

Vallisneri, M., et al., LOSC, Proc. 10th LISA Symp., U Florida, May 18-23, 2014; arXiv:1410.4839

van Putten, M.H.P.M., 1999, Science, 284, 115

van Putten, M.H.P.M., 2001, Phys. Rev. Lett., 87, 091101

van Putten, M.H.P.M., & Levinson, A., 2002, Science, 295, 1874

van Putten, M.H.P.M., & Levinson, A., 2002, Class. Quant. Grav., 19, 1309

van Putten, M.H.P.M., & Levinson, A., 2003, ApJ, 584, 937

van Putten, M.H.P.M., 2012, Prog. Theor. Phys., 127, 331

van Putten, M.H.P.M., Guidorzi, C.. & Frontera, F.. 2014, ApJ, 786, 146

van Putten, 2015, ApJ, 810, 7

van Putten, M.H.P.M. & Della Valle, M., 2019, MNRAS, 482, L46

Wald, R.M., 1984, General Relativity, University of Chicago Press

Yang, H., East, W.E., & Lehner, L., 2018, ApJ, 856, 110

Yu Y.-W., Liu, L.-D., & Dai, Z.-G., 2018, ApJ, 861, 114